Journal of the European Ceramic Society **11** (1993) 463–469

Efficient Grinding of Ce-TZP with SiC Wheels

V. E. Annamalai,[a] T. Sornakumar,[b] C. V. Gokularathnam[a] & R. Krishnamurthy[b]

[a] Department of Metallurgical Engineering, [b] Department of Mechanical Engineering,
Indian Institute of Technology, Madras 600036, India

(Received 28 May 1992; revised version received 3 September 1992; accepted 28 September 1992)

Abstract

Transformation toughened zirconia has been widely studied. Most of the reports on zirconia deal only with the transformation behaviour in various environments. However, for the effective use of any ceramic, information on processing is essential. In spite of stabilized zirconia being an important material for various technical applications, details on how it can be processed by grinding is lacking. The present paper reports on the grindability of ceria-stabilized zirconia with various grinding wheels. Based on the grinding forces, specific grinding energies, phase structure and grinding induced surface cracks, it is shown that SiC grinding wheels can grind Ce-TZP efficiently.

Umwandlungsverstärktes Zirkoniumdioxid ist Gegenstand zahlreicher Untersuchungen gewesen. Die meisten veröffentlichten Arbeiten über Zirkoniumdioxid behandeln nur das Umwandlungsverhalten in verschiedenen Umgebungen. Für den effektiven Einsatz keramischer Werkstoffe sind Informationen über die Verarbeitung unerläßlich. Obwohl stabilisiertes Zirkoniumdioxid einen wichtigen Werkstoff für viele technische Anwendungen darstellt, fehlen detaillierte Informationen über die Möglichkeiten der Bearbeitung durch Schleifen. Diese Arbeit befaßt sich mit der Schleifbarkeit von Ceriumdioxid stabilisiertem Zirkoniumdioxid mit verschiedenen Schleifrädern. Ausgehend von den Schleifkräften, den spezifischen Schleifenergien, der Phasenstruktur und durch das Schleifen induzierten Oberflächenrissen wird gezeigt, daß mit SiC Schleifrädern Ce-TZP sehr effizient geschliffen werden können.

Le renforcement de la zircone par transformation de phase a été largement étudié. La plupart des travaux s'intéressent au phénomène de transformation proprement dit dans divers environnements, cependant, pour l'utilisation efficace de toute céramique, une information quant aux paramètres régissant son élaboration est essentielle. En dépit de l'importance de la zircone partiellement stabilisée en tant que matériau pour diverses applications techniques, les détails sur son usinage sont manquants. Cet article traite de l'usinabilité de la zircone stabilisée à l'oxyde de cérium avec diverses meules d'usinage. En se basant sur les forces mises en jeu, les énergies spécifiques, la structure des phases et les défauts induits en surface, le tout lors de l'usinage, on démontre que les meules à base de SiC satisfont efficacement à cette opération pour les Ce-TZP.

1 Introduction

Usually TZP (tetragonal zirconia polycrystal) materials (as well as most other ceramic materials) are fabricated through powder processing techniques such as compaction and sintering. Compaction in dies restricts the complexity of the parts that can be produced. It is a general practice to produce a sintered product with sufficient allowance for sintering shrinkage and for further machining. So, machining the sintered piece is a common feature in most cases, either for imparting a shape change, for obtaining a near-net shape, or for attaining a desired level of surface finish. Grinding with a diamond wheel has been established as an effective method of machining sintered ceramics.[1] The problem of grinding ceramics, which are hard and brittle, has been addressed in detail by Inasaki.[2,3]

In the present study, Ce-TZP (ceria-TZP), has been ground with diamond, CBN (cubic boron nitride) and SiC (silicon carbide) wheels and their relative performance is assessed.

2 Fabrication

Specimens of size 14 mm × 14 mm × 4 mm were prepared by dry pressing 12 mol% ceria-stabilized

Journal of the European Ceramic Society 0955-2219/93/$6.00

Table 1. Grinding conditions

Machine	Tool and cutter grinder
Operation	Surface grinding
Grinding wheel	Diamond—BZ 1A1-100-6-1-6 (100 mm diameter, 6 mm width, grit size 185) CBN—B 120 RR 100 D (152 mm diameter, 6·4 mm width, grit size 120) SiC—GC 60-K5-VG (137·8 mm diameter, 12·5 mm width, grit size 60)
Wheel speeds	1100, 2200, 3000 and 6000 rpm
Depths of cut	10, 20, 30 and 40 microns
Work feed rate	27·5 mm/min
Coolant	No coolant (dry grinding)

zirconia powder (Tosoh, Japan, TZ-12Ce) with a suitable binder and sintering at 1350°C for 2 h. The sintered surface had 100% tetragonal (t) phase.[4]

3 Experimental

Grindability studies were conducted on these specimens, with diamond, CBN and SiC grinding wheels under the conditions shown in Table 1.

The tangential and normal force components were measured for various grinding velocities and depths of cut, with the help of a Kistler dynamometer. The grinding chips were collected on double-sided adhesive tape pasted onto glass plates. The surface finish values of the ground surfaces were assessed with the help of a perthometer Mahr-Perthen, Germany). Both the ground surfaces and the collected chips were analysed by XRD to assess the extent of phase transformations. The ground surfaces were also characterized by optical microscopy.

4 Observations

4.1 Grinding with diamond wheel

Table 2 shows the force values measured during grinding with diamond wheel. It can be seen that the normal and tangential grinding forces exhibit a totally different trend, i.e. when one increases with grinding speed, the other decreases and vice versa. However, it is the tangential force that is required for specific grinding energy calculations.[5] Accordingly, using the tangential force, the specific grinding energies calculated for various grinding conditions are listed in Table 3. A specimen calculation for specific grinding energy is shown in the Appendix.

In general, the specific grinding energy increases with decreasing depth of cut[5] and it is of a high value for slow removal rates.[6] Slow removal rates refer to higher grinding speeds, because, at constant work feed rate, the chip volume removed per cut will decrease as wheel speed increases. Similar trends can be seen in Table 3 wherein the specific grinding energy increases with decreasing depth of cut and for a given depth of cut, increases with increasing grinding speeds (i.e. slow removal rates). However, the increase in tangential grinding force at any given speed is observed only up to 30 microns depth of grinding, beyond which there is a drop in tangential grinding force.

From Table 2, it is clear that the tangential force is a minimum for the grinding velocity of 11·51 m/s and is a maximum for a grinding velocity of 15·7 m/s. Table 2 also shows the influence of depth of cut on the tangential force, for various speeds. It can be seen that a depth of cut of 30 microns always results in a higher force value.

Table 2. Forces during grinding with diamond wheel

Grinding		*Tangential force (N) depth of grinding*				*Normal force (N) depth of grinding*			
Speed (rpm)	*Velocity (m/s)*	*10*	*20*	*30*	*40*	*10*	*20*	*30*	*40*
1100	5·76	6	7	8	7	5	7	10	13
2200	11·51	4	5	6	4	6	9	12	14
3000	15·70	8	11·5	12	9	3·5	4	11	12
6000	31·40	7	8	9	8	7	9	10	11

Table 3. Specific grinding energies for grinding with diamond wheel

Grinding velocity (m/s)	*Specific grinding energy (GPa)*			
	Depth of grinding (microns)			
	10	*20*	*30*	*40*
5·76	1256	733	558	366
11·51	1675	1047	837	419
15·70	4567	3283	2284	1285
31·40	7992	4567	3425	2284

Table 4. Forces during grinding with CBN wheel

Grinding		*Tangential force (N)*			
Speed (rpm)	*Velocity (m/s)*	*Depth of grinding (microns)*			
		10	*20*	*30*	*40*
1 100	8·78	1	2	3·5	2
2 200	17·56	2	3·5	4	3·5
3 000	23·94	1·25	1·5	2	1·5
6 000	47·88	1	1·25	1	0·75

Table 5. Specific grinding energies for grinding with CBN wheel

Grinding velocity (m/s)	*Specific grinding energy (GPa)*			
	Depth of grinding (microns)			
	10	*20*	*30*	*40*
8·78	299	299	349	150
17·56	1 197	1 048	798	524
23·94	1 020	612	544	306
47·88	1 632	1 020	544	306

4.2 Grinding with CBN wheel

Grinding studies were conducted on Ce-TZP samples with a CBN wheel. The experimental procedure was exactly similar to that of diamond grinding. The conditions of grinding are as shown in Table 1. It may be noted that even though the spindle speeds are the same, the grinding velocities for different wheels are different due to the difference in their diameters. Thus a speed of 1100 rpm leads to a velocity of 5·76 m/s for the diamond wheel (diameter 100 mm) whereas it leads to 8·78 m/s for the CBN wheel (diameter 152 mm). Table 4 shows the tangential grinding forces for various conditions of grinding. It can be seen that for any given depth of cut, 17·56 m/s always shows a higher value. It is of interest to note that this very close to the value of 15·76 m/s which always resulted in a higher force value for grinding with the diamond wheel. Also, as in the diamond wheel grinding, a depth of cut of 30 microns always results in a higher force value. The specific grinding energies are shown in Table 5. Here too, as in the diamond wheel grinding, at any given depth of cut, the tangential grinding force increases up to a depth of grinding of 30 microns and then drops with further increase in depth of grinding.

4.3 Grinding with SiC wheel

Normally, since ceramics are hard and brittle, they are ground only with diamond or CBN grinding wheels. But in the present case, the hardness of Ce-TZP is less than that of other ceramics, the actual value[4-7] being less than 900 H_v. So, other wheels like SiC and alumina, which are less hard than diamond or CBN, may be tried on Ce-TZP.

Both alumina and SiC wheels were tried. Alumina was found to glaze out and could not perform any grinding of Ce-TZP. SiC could grind well. The same grinding experiments as for CBN were carried out with the SiC wheel (Table 1). The tangential grinding force and the specific grinding energy values are shown in Tables 6 and 7 respectively. As in the previous two cases, the SiC wheel also shows an increase in the tangential grinding force up to a depth of grinding of 30 microns and then drops with further increase in depth of grinding.

Table 6. Forces during grinding with SiC wheel

Grinding		*Tangential force (N)*			
Speed (rpm)	*Velocity (m/s)*	*Depth of grinding (microns)*			
		10	*20*	*30*	*40*
1 100	7·95	6	8	14	13·5
2 200	15·9	3·5	5·5	7	6
3 000	21·7	4·5	5	6	5·5
6 000	43·4	1	2	2·5	1·5

Table 7. Specific grinding energies for grinding with SiC wheel

Grinding velocity (m/s)	*Specific grinding energy (GPa)*			
	Depth of grinding (microns)			
	10	*20*	*30*	*40*
7·95	548	365	426	308
15·9	639	502	426	273
21·7	1 121	623	498	343
43·4	4 983	498	415	187

4.4 Relative performance

The relative performance of the three wheels is assessed as follows. The force values are compared in Fig. 1 and the surface roughness (R_a) values are compared in Fig. 2.

From these figures, it can be seen that CBN exerts less force and produces surfaces of a higher roughness value. The force values fluctuate between the SiC and diamond wheels but the surface finish attainable with the SiC wheel is generally better than with the other two wheels. However, in terms of specific grinding energy, CBN and SiC exert very low specific grinding energies compared to that of diamond (about one fourth to one sixth that of diamond).

In general, grinding wheels made up of abrasives of finer grits produce a better surface finish[8] and a large number indicates a finer grit size.[9] Accordingly, from Table 1, SiC, CBN and diamond are in increasing order of fineness of grit (grit size numbers being 60, 120 and 185, respectively). In spite of having coarser grits than the diamond and CBN wheels, the SiC wheel is capable of producing a better finish.

5 Transformations during Grinding

Grinding involves both stress and temperature.[10] Hence, the combined effect of grinding on the transformation of tetragonal zirconia has been the topic of many studies[11–14] Swain & Hannink[15] have conducted detailed studies on the nature of transformation in Ce-TZP during grinding. They have conducted grinding studies at one fixed speed (2800 rpm) and one fixed depth of cut (15–25 microns). Based on this work, they have concluded that Ce-TZP responds to machine grinding by a cyclic t–m–t transformation.

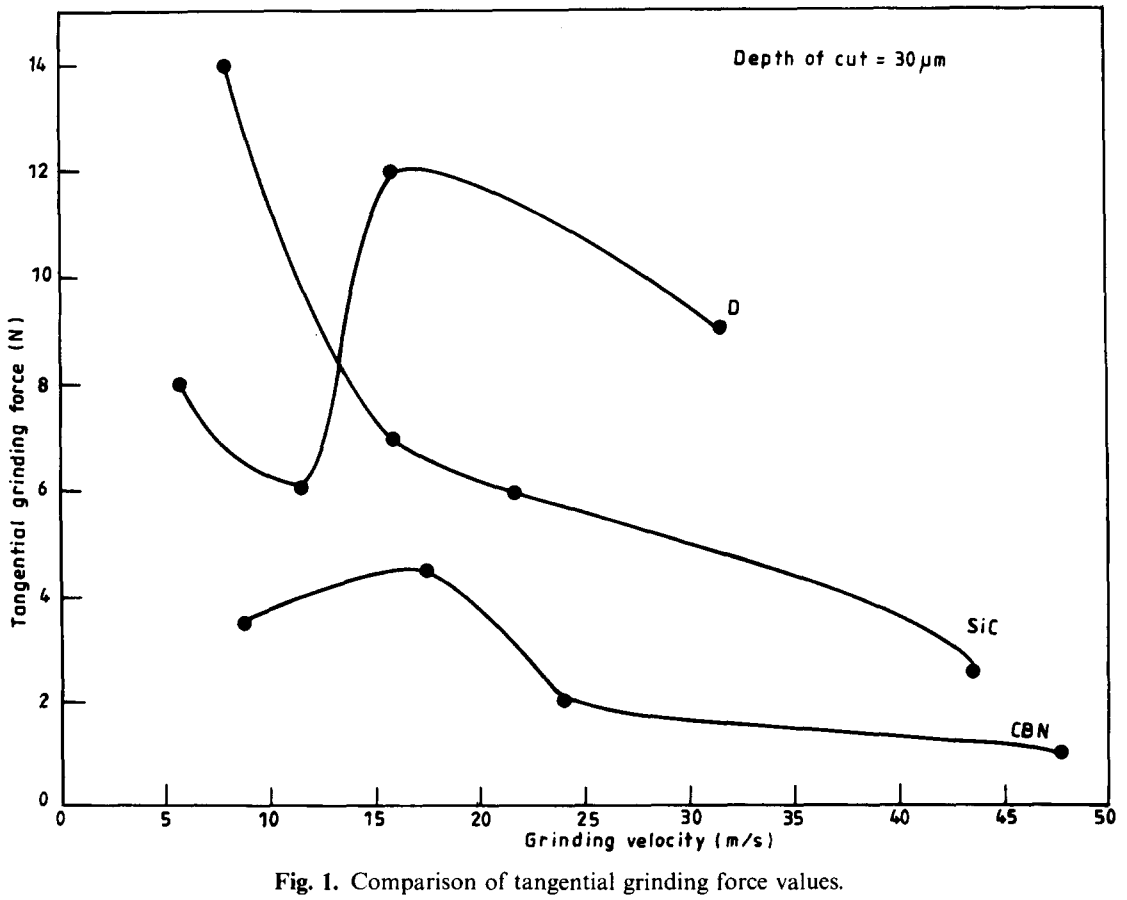

Fig. 1. Comparison of tangential grinding force values.

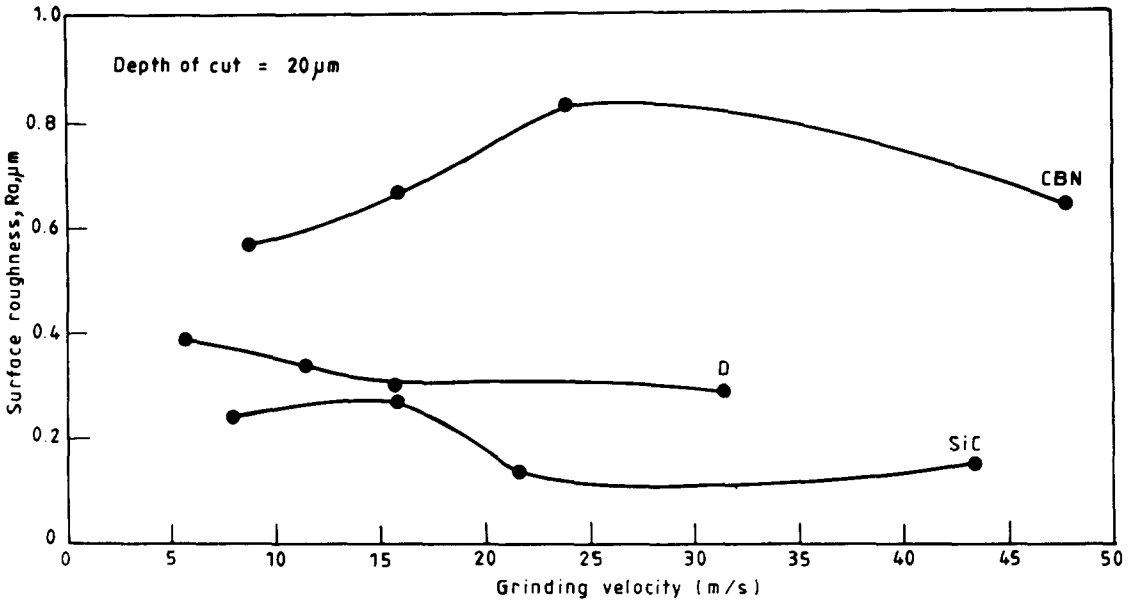

Fig. 2. Comparison of surface finish R_a values.

Table 8. Phase content of the ground surface and grinding chips

Sample	*Wheel speed (rpm)*	*Percentage tetragonal phase*		*Nature of transformation*
		Surface	*Chip*	
1	1 100	78	56	(t–m)
2	2 200	0	100	(t–m)
3	3 000	100	100	(t–m–t)
4	6 000	64	100	(t–m–t–m)

Depth of cut = 40 microns. Diamond grinding wheel.

But the transformation response of Ce-TZP to machine grinding is very much dependent on the combined effects of stress and temperature. Any desired combination of stress and temperature can be attained by varying the grinding parameters. Accordingly, the present authors have shown that during grinding with a diamond wheel, there are three distinct stages of transformation, as shown in Table 8. At lower grinding speeds, only the mechanical stress induced t–m transformation is observed. As the grinding speed increases, the frictional heat serves to revert the m-phase (produced by stress) back to the t-phase. When the speed increases enormously, a third stage of thermal stress induced t–m transformation is observed. A detailed analysis of these transformations and a possible mechanism have been reported elsewhere.[16] These transformations generally result in what is called asperity folding. Asperity folding refers to the folding of the displaced edges of a groove, probably by plastic deformation, resulting in smooth transition from peak to trough of every groove. Such an asperity folding, as shown in Fig. 3, smooths the ground surface. Similar asperity folding has been reported[17] during grinding of Y-TZP (yttria-TZP).

For both SiC and CBN wheels, the ground surfaces and chips of Ce-TZP showed 100% t-phase for all conditions of grinding. Phase analysis was performed using the expression of Torayo *et al.*[18]

6 Correlation between the Surface Cracks and Phase Structure

It has been observed that irrespective of the type of wheel, ground surfaces showing 100% t-phase

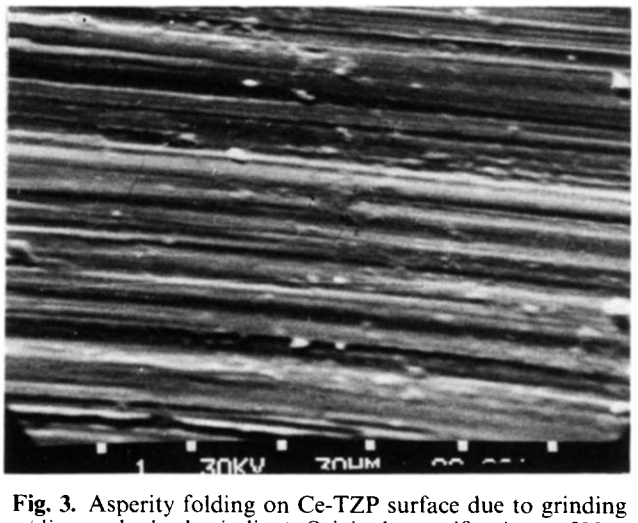

Fig. 3. Asperity folding on Ce-TZP surface due to grinding (diamond wheel grinding). Original magnification × 500.

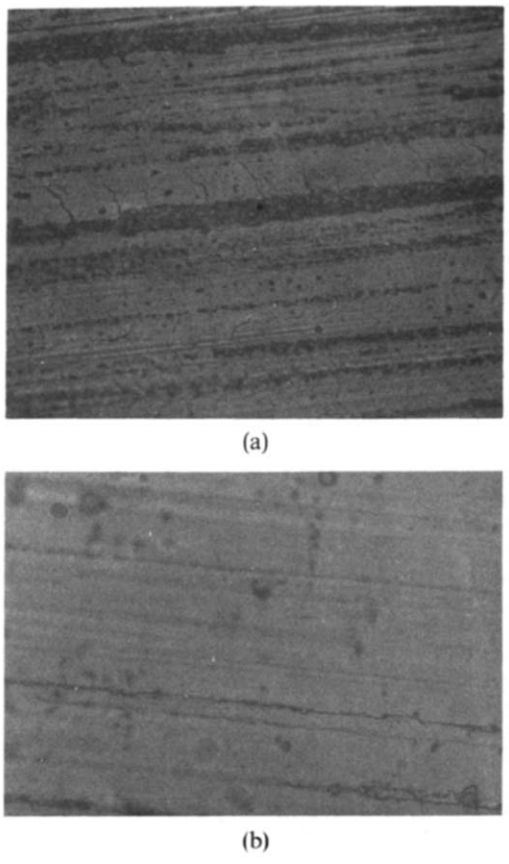

Fig. 4. Grinding induced surface cracks on Ce-TZP due to (a) diamond wheel grinding and (b) SiC wheel grinding. Magnification ×375.

always exhibit a similar crack pattern on the ground surface. The cracks appear to have the shape of a coiled telephone wire, just pulled apart, thereby showing some opened out loops. These have been dealt in greater detail in another report.[16] This can be appreciated by comparing Fig. 4(a) and (b). Figure 4(a) represents the surface ground with the diamond grinding wheel and exhibiting 100% t-phase. Figure 4(b) is the surface ground with the SiC wheel, exhibiting 100% t-phase. The similarity between these two figures is an indication that this is the type of surface crack which corresponds to the complete cyclic (t–m–t) transformation. Surfaces ground with CBN also had similar appearance.

7 Chip Analysis

When observed under a microscope, the chips are slightly flaky and continuous (in all the three cases), as those produced during turning or drilling of metallic materials. This is an indication that the material is plastically deformed, before being removed as chip.

8 Conclusions

Ce-TZP has been ground with diamond, CBN and SiC grinding wheels.

(1) The SiC wheel is observed to produce a better finish with about one fourth to one sixth of the specific grinding energy of that of the diamond wheel.
(2) Unlike the diamond wheel, CBN and SiC wheels always result in 100% t-phase on the surface, thereby leaving the surface phase structure unaltered.
(3) Irrespective of the type of wheel used, surfaces of Ce-TZP showing 100% t-phase after grinding always show a striking similarity in the crack patterns of the ground surface.
(4) Whatever the type of wheel used for grinding Ce-TZP, the variation of specific grinding energy with depth of grinding is always similar.

References

1. Kobayashi, A., Recent development in diamond wheel grinding. *Annals of the CIRP*, **18** (1970) 31–47.
2. Inasaki, I., Grinding of hard and brittle materials. *Annals of the CIRP*, **36**(2) (1987) 463–71.
3. Inasaki, I., High efficiency grinding of advanced ceramics. *Annals of the CIRP*, **36**(1) (1986) 211–14.
4. Annamalai, V. E., Gokularathnam, C. V. & Krishnamurthy, R., On the sintering behaviour of 12 mol% ceria stabilized zirconia. *J. Mater. Sci. Lett.*, **11** (1992) 642–44.
5. Dieter, G. E., In *Mechanical Metallurgy*. McGraw Hill, Singapore, 1986, pp. 702.
6. Malkin, S., *Grinding Technology, Theory and Application of Machining with Abrasives*. Ellis Horwood Ltd, Chichester, London, 1989, pp. 118–24.
7. Tsukuma, K., Mechanical properties and thermal stability of CeO_2 containing tetragonal zirconia polycrystals. *Amer. Ceram. Soc. Bull.*, **65**(10) (1986) 1386–9.
8. Malkin, S., In *Grinding Technology, Theory and Application of Machining with Abrasives*. Ellis Horwood Ltd, Chichester, London, 1989, pp. 252.
9. Malkin, S., In *Grinding Technology, Theory and Application of Machining with Abrasives*. Ellis Horwood Ltd, Chichester, London, 1989, pp. 20.
10. Bhattacharyya, A., *Metal Cutting Theory and Practice*. Central Book Publishers, Calcutta, India, 1984, pp. 477.
11. Hill, R. J., Howard, C. J. & Reichert, B. E., Quantitative phase abundance in Mg-PSZ by Reitveld analysis of neutron and X-ray diffraction data. In *Ceramic Developments*, ed. C. C. Sorrell & B. Ben-Nissan. Trans Tech Publications, Switzerland, 1988, pp. 159–63.
12. Swain, M. V., Grinding induced tempering of ceramics containing metastable tetragonal zirconia. *J. Mater. Sci.*, **15**(6) (1980) 1577–9.
13. Gross, V. & Swain, M. V., Mechanical properties and microstructure of sintered and hot isostatically pressed yttria partially stabilized zirconia. *J. Amer. Ceram. Soc.*, **22** (1986) 1–12.
14. Virkar, A. V. & Matsumoto, R. L. K., Ferroelastic domain switching as a toughening mechanism in tetragonal zirconia. *J. Amer. Ceram. Soc.*, **69**(10) (1986) C-224–C-226.
15. Swain, M. V. & Hannink, R. H. J., Metastability of the martensitic transformation in a 12 mol% ceria–zirconia alloy: II. Grinding studies. *J. Amer. Ceram. Soc.*, **72**(8) (1989) 1358–64.
16. Annamalai, V. E., Sornakumar, T., Gokularathnam, C. V. & Krishnamurthy, R., Transformations during grinding of Ce-TZP. *J. Amer. Ceram. Soc.*, **75** (1992) 2559–64.

17. Krishnamurthy, R., Arunachalam, L. M., Gokularathnam, C. V. & Venkatesh, V. C., Grinding of transformation-toughened Y-TZP ceramics. *Annals of the CIRP*, **40** (1991) 331–3.
18. Torayo, H., Yoshimura, M. & Somiya, S., Calibration curve for quantitative analysis of the monoclinic–tetragonal ZrO_2 system by X-ray diffraction. *J. Amer. Ceram. Soc.*, **67** (1984) C-119–C-121.

Appendix—Calculation of Specific Grinding Energy

Specimen calculation for 5·76 m/s and 10 microns depth of cut.

Tangential force = 6 N
Depth of cut = 10 microns
= 10/1000 mm
Wheel speed = 5·76 m/s
Work speed = 27·5 mm/min
= (27·5/1000)/60 m/s
Wheel width = 6 mm

$$\text{Specific grinding energy} = \frac{(\text{Tangential force}).(\text{Wheel speed})}{(\text{Work speed}).(\text{Wheel width}).(\text{Depth of cut})}$$

$$\text{Units} = \frac{(\text{Kgf}).(\text{m/s})}{(\text{m/s}).(\text{mm}).(\text{mm})} \times 9{\cdot}806 \times 10^6\ \text{Pa}$$

$$= \frac{(\text{N}).(\text{m/s})}{(\text{m/s}).(\text{mm}).(\text{mm})} \times 10^6\ \text{Pa}$$

since Kgf/9·806 = N.
Hence

$$\text{Specific grinding energy} = 6 \times 5{\cdot}76 \times \frac{60 \times 1000}{27{\cdot}5} \times \frac{1000}{10} \times \frac{1}{6} \times 10^6\ \text{Pa}$$

$$= 1{\cdot}256 \times 10^6 \times 10^6\ \text{Pa}$$
$$= 1{\cdot}256 \times 10^3 \times 10^9\ \text{Pa}$$
$$= 1256 \times 10^9\ \text{Pa} = 1256\ \text{GPa}$$